

Computation of Trailing-Edge Noise Using a Zonal RANS-LES Approach and Acoustic Analogy

Fabrice Mathey

Fluent France, 1 place Charles de Gaulle, 78180 Montigny Le Bretonneux, France
fabrice.mathey@fluent.fr

ABSTRACT

This paper document the evaluation of a zonal RANS-LES approach for the prediction of broadband and tonal noise generated by the flow past an airfoil trailing edge at a high Reynolds number. A multi-domain decomposition is considered, where the acoustic sources are resolved with a LES sub-domain embedded in the RANS domain. At the RANS-LES interface, a stochastic vortex method is used to generate synthetic turbulent perturbations. The far-field noise is calculated using the aeroacoustic analogy of Ffowcs-Williams and Hawkings. The results of the simulation are compared with available acoustic and mean velocity measurements. The investigation demonstrates the ability of this approach to predict the aerodynamic and aeroacoustic properties of the flow. Two simulations are performed in order to address the sensitivity of the results to the perturbation model. The comparison clearly indicates the critical influence of the model.

INTRODUCTION

This study deals with numerical prediction of airfoil trailing edge noise. Trailing-edge aeroacoustics is of importance in both aeronautical and naval applications. The dipole sound produced by the edge scattering of pressure fluctuations at a trailing edge is most often an undesirable effect. These pressure fluctuations are created by turbulent eddies as they convect over the trailing edge. This causes edge scattering of noise to the far field. This scattering mechanism can produce strong broadband and/or tonal noise which is radiated to the far field.

In this work, an Hybrid zonal RANS/LES unsteady CFD simulation is used to get a prediction of the acoustic sources, which are then use as an entry data of an acoustic propagation model. The case under study corresponds to the recent experiment conducted by Kunze [1]. The trailing edge shape considered is identical with on of the trailing edge shapes previously investigated by Blake [2]. The accurate prediction of such a high Reynolds number flow requires computational resources which are beyond the capabilities of “usual” computers. In this paper, a zonal RANS/LES method is proposed to perform the numerical predictions of aerodynamic noise sources at a moderate computational cost. The idea is to restrict the expensive LES calculation to the aeroacoustic source regions, while the rest of the configuration can be treated by a much cheaper RANS approach. The sound propagation is handled by a specific numerical tool (a Ffowcs-Williams Hawking acoustic analogies for instance).

Previous authors [3,4] have proposed such a zonal RANS/LES technique. These approaches all share a common issue, namely the definition of appropriate RANS to LES interface conditions. Several techniques can be considered. For example precursor domains or recycling methods are probably the most accurate techniques that can be considered. However the

generalization to arbitrary complex 3D geometries presents some significant challenges.

In this paper, an alternative synthetic generator is considered. The Vortex Method (VM hereafter) from Sergent [5] is used to reconstruct the turbulent fluctuations at the RANS/LES interface. Extensive validations [5,6] have shown that the VM offers a relative inexpensive and accurate way to generate random fluctuations representing a turbulent flow field at the inlet of a LES domain. In the current study, the method is adapted for an embedded LES sub-domain inside an RANS domain. Moreover, the influence of the model is addressed in the specific context of acoustic sources prediction.

METHODOLOGY

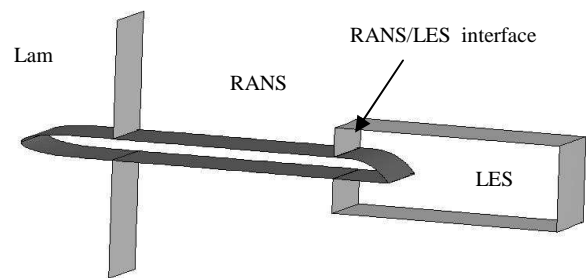


Figure 1: Experimental setup, computational domain and RANS & LES sub-domains

The flow configuration is shown in Figure 1. A flat airfoil with an elliptical leading edge and an asymmetric 45° rounded trailing edge is placed in a uniform stream. The Reynolds number based on the free-stream velocity U_{inf} and the chord is $1.8 \cdot 10^6$. Two microphones are attached to a boom and are placed at 1.83m away from the trailing edge. The computational domain is decomposed into a quasi 2D laminar sub-domain, a quasi 2D turbulent RANS

sub-domain and a non-conformal LES sub-domain embedded inside the RANS domain, as shown in Figure 1. The laminar zone is considered to trigger the transition of the boundary layer. In the experiment, the transition of the boundary layer is triggered at 25% of the chord length on both sides of the model. At the RANS/LES interfaces where the grid is suddenly refined, the turbulent viscosity model switch from RANS to LES. At this interface, as the modelled RANS Reynolds stress is vanishing, the LES requires the generation of explicitly resolved turbulent eddies. In order to construct these time-dependent inlet conditions, a random 2D vortex method is considered. With this approach, a perturbation is added to the mean velocity via a fluctuating two-dimensional vorticity field (two-dimensional in the plane normal to the streamwise direction). The vortex method is based on the Lagrangian form of the 2D evolution equation of the vorticity and the Biot-Savart law. A particle discretization is used in order to solve this equation. These particles or ‘‘vortex points’’ are convected randomly and carry information about the vorticity field. If N is the number of vortex points and S the area of the inlet section, the amount of vorticity carried by a given particle i is represented by the circulation Γ_i and an assumed spatial distribution η :

$$\Gamma_i(x) = 4 \sqrt{\frac{\pi S k(x)}{3N(2\ln(3) - 3\ln(2))}} \quad (1)$$

$$\eta(x) = \frac{1}{2\pi\sigma^2} \left(2e^{-\frac{|x|^2}{2\sigma^2}} - 1 \right) e^{-\frac{|x|^2}{2\sigma^2}} \quad (2)$$

where k is the turbulence kinetic energy. The parameter σ provides control over the size of a vortex particle. The resulting discretization for the velocity field is thus given by:

$$\vec{u}(\vec{x}) = \frac{1}{2\pi} \sum_{i=1}^N \Gamma_i \frac{(\vec{x}_i - \vec{x}) \times \vec{z}}{|\vec{x}_i - \vec{x}|^2} \left(1 - e^{-\frac{|\vec{x}_i - \vec{x}|^2}{2\sigma^2}} \right) e^{-\frac{|\vec{x}_i - \vec{x}|^2}{2\sigma^2}} \quad (3)$$

Originally in Sergent [5], the size of the vortex was fixed by an ad-hoc value of σ . In order to make this method generally applicable, a local vortex size is specified through a turbulent mixing length hypothesis. Consequently, σ is calculated from the known profiles of mean turbulence kinetic energy and mean dissipation rate at the inlet according to:

$$2\sigma = ck^{3/2} / \epsilon \quad (4)$$

where $c=0.16$. In order to ensure that the vortex always belongs to the resolved scales, the minimum value of σ in Eqn. 4 is bounded by the local grid size. The sign of the circulation of each vortex is changed randomly after a characteristic turbulent time scale τ has passed. In the present work, a simplified linear kinematic model is considered for the stream wise velocity fluctuations. This model mimics the influence of the 2D vortex on the stream-wise mean velocity field. This approach combines the advantages of preserving fully spatial coherence of the

vortex and being independent of τ contrary to the stochastic model originally suggested by Sergent [5]. If the mean stream-wise velocity U is considered as a passive scalar, the fluctuation u' resulting from the transport of U by \vec{v}' (where \vec{v}' is the planar fluctuating 2D velocity field as computed by the VM) can be modelled by $u' = -\vec{v}' \cdot \vec{g}$ where \vec{g} is the unit vector aligned with the mean inlet velocity gradient $\overline{\nabla U}$. When this mean velocity gradient is equal to zero, a random perturbation can be considered instead.

Virtual body forces are employed in the momentum equations to add the reconstructed turbulent fluctuations to the velocity field. These virtual body forces are considered only in the first LES cells close to the RANS/LES interfaces

The RANS-SST model [7] is used in the RANS region, and the Smagorinsky [11] model is considered in the refined LES grid region. The grid used for the simulation is shown in Figure 2. The wall resolution in wall units is $y^+ = 1$ along the airfoil, both in the RANS and in the LES region. The mesh is coarsened in the RANS zone in the other directions.

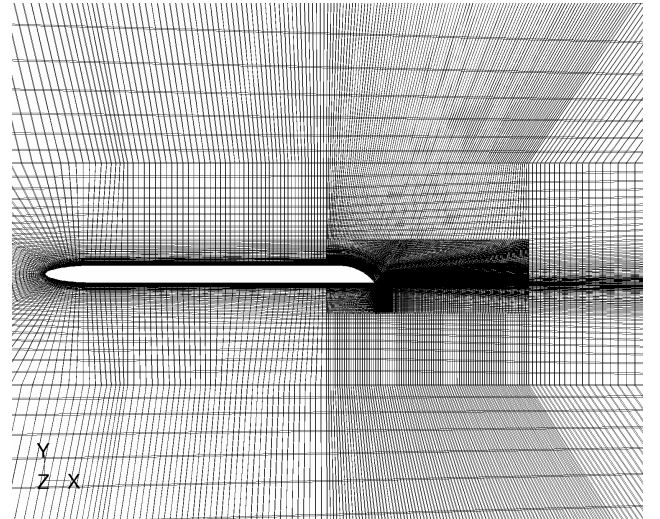


Figure 2: 2D slice of the computational grid with the embedded LES refined grid.

The total number of grid points is nearly equal to 1.5×10^6 , the LES part corresponding to 1.4×10^6 . In the LES subdomain, the mesh is stretched in the stream-wise and wall normal directions, and is uniform in the spanwise direction with 100 cells. The spanwise extent of the computational domain is equal to 20% of the chord. It is assumed that the fluctuating field is periodic in the spanwise direction. The compressible simulation is performed with FLUENT [8] general-purpose unstructured control-volume code. The unsteady LES run uses a second-order implicit scheme for temporal discretization and second order central differencing for spatial discretization. The details of the finite-volume method are described by Mathur and Murthy [9]. The numerical aspects relevant to the implementation of the LES are described in [10] The subgrid-scale stress models used in this study is the Smagorinsky model [11]. Two

different simulations (hereafter referred as to as RUN1 and RUN2) are performed. The first simulation RUN1 is performed with a random forcing (white noise) at the RANS/LES interface. The random noise is considered here in order to address the sensitivity of the results to the accuracy of the turbulent forcing. White noise is known to produce poor results due to the non-correlated nature of the signal. On the contrary, the perturbation generated by the Vortex Method is temporally and spatially correlated. This is an important requirement to ensure that the synthetic turbulent field can be sustained. The second simulation RUN2 is performed with this Vortex Method.

RESULTS AND DISCUSSION

Aerodynamic simulation

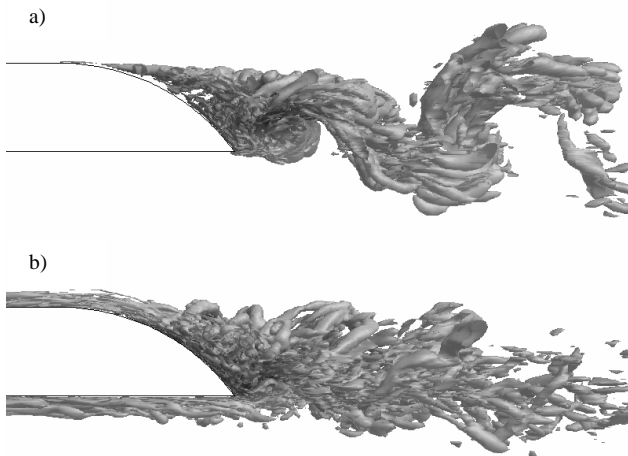


Figure 3: Visualization of the Q -criterion in the wake of the airfoil. Isosurface $Q=500 \times 10^5$ colored by the streamwise velocity: a) RUN1 b) RUN2.

A qualitative overview of the flow is given in Figure 3 for the two RANS/LES simulations. Both cases show the fully-developed 3D flow. The upper boundary layer separates gradually in the adverse pressure gradient created by the rounded edge, while the lower boundary layer separates instantly at the sharp edge. The vorticity shed into the flow from the boundary layers is convected downstream creating a von Karman street. The main shedding can be recognized by oscillations in the wake of the blade. These oscillations are much more pronounced for the simulation without the turbulent forcing. The effect of the turbulent forcing on the instantaneous flow is also visible in Figure 3. The turbulent eddies generated at the RANS/LES interface are convected downstream and delay the separation of the boundary layer. These eddies interact with the coherent structures generated past the separation points. This interaction results in an early transition of the separated shear layer to a fully 3D state.

The position of the mean separation points are compared in Table 1. A good agreement is found between RUN2 and the experimental data, whereas in RUN1 the separation is predicted farther upstream.

Time-averaged mean streamwise velocity profiles and streamwise rms fluctuations in the wake are given in

Figure 4. Both quantities are reasonably well predicted by RUN2. The velocity deficits are slightly over-predicted in the far wake, and the rms-values are slightly over-predicted on the upper boundary layer side. However RUN1 considerably under-predict the mean velocity profiles deficit already in the near wake, and considerably over-predict the velocity fluctuations. Both profiles are also shifted to upper boundary layer side, as a result of the early separation of the upper boundary layer predicted by RUN1.

Table 1: Distance (on the x -axis) of the upper boundary layer separation point from the trailing edge.

Simulation	Distance
RUN1	75 mm
RUN2	45 mm
EXP	35 mm

Aeroacoustic prediction

Based on the work of Ffowcs-Williams and Hawkins [13], the far-field noise is calculated by applying the aeroacoustic analogy to the rigid wall surface of the airfoil as the integration surface. The spectra presented above are obtained by a FFT with a length of 10 000 points and the use of Hanning-window. The simulated span $L_s=0.2c$ being less than the span of the test configuration $L_{exp}=0.67c$, a level correction is applied to the simulated spectra [13].

Figure 5 shows the RANS/LES results in comparison with measurements. The simulation using the VM (RUN2) is in a general good agreement with the broadband spectrum based on the measurements. The level of the main tonal peak (at 220Hz) is well predicted, although the simulation slightly over-predicts the frequency (250 Hz). It is particularly noteworthy that the simulation performed with the white noise (RUN1) over-predicts the amplitude of the tonal peak, and under-predict its frequency. The broadband is also more accurately predicted by RUN2, while RUN1 under-predict the level both at the low and high frequency range.

It was shown by Shannon and Morris [14] that the tonal noise results from the large scale coherent structures generated at the separation points. The unsteady surface pressure generated on the surface by these motions is responsible for the acoustic scattering which produces the tonal noise at the vortex shedding frequency. In simulation RUN2, the VM synthetic turbulent perturbation delays the separation point compared to RUN1. This results in a narrower wake as shown by the visualization of the flow and the mean velocity profiles, and explains the increase of the vortex shedding frequency. Finally, interaction between the generated synthetic turbulence and the detached eddies which enhances the momentum transport and the transition to 3D modes may explain the damping of the tonal noise and general higher level of broadband noise.

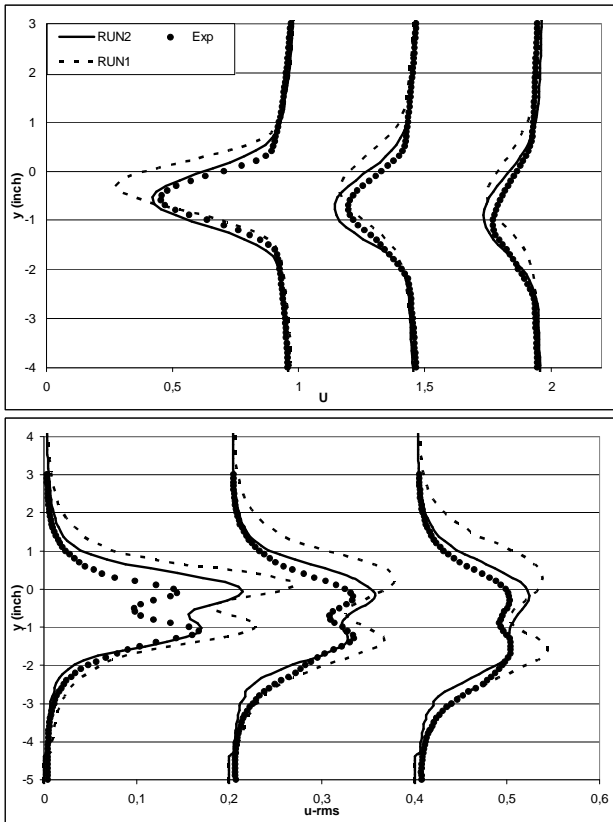


Figure 4: Comparison of Mean streamwise velocity and mean streamwise rms velocity in the wake for $x=20$ inch, $x=22$ inch and $x=24$ inch. Measurements from Kunze [1].

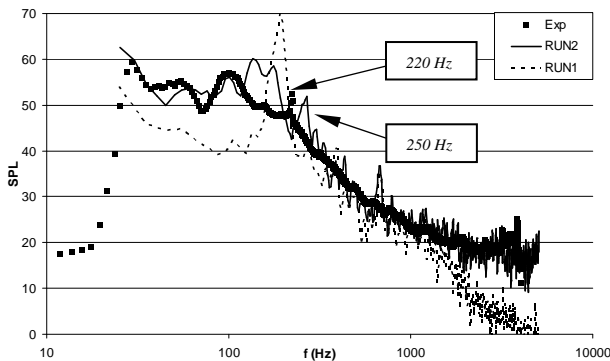


Figure 5: Comparison of the SPL of the far-field radiated sound for an observer located at a normal distance of 1.83 m from the trailing edge. Measurements from Kunze [1].

CONCLUSION

In this work a zonal RANS-LES simulation has been proposed to study the aeroacoustic trailing edge noise. This technique was shown to accurately predict the aeroacoustic source for a high Reynolds number flow at an affordable cost. It was shown that the synthetic turbulent perturbation generated by the Vortex Method at the RANS/LES interface allows to reproduce correctly both the aerodynamic and aeroacoustic properties of the trailing edge flow, with an accurate prediction of the separation and of the radiated sound. Two simulations were performed in order to address the sensitivity of the results to the RANS-LES interface model. The

comparison clearly indicated the critical influence of the model.

BIBLIOGRAPHY

- [1] Kunze C. "Acoustic and Velocity Measurements in the Flow Past an Airfoil Trailing Edge". Master Thesis, University of Notre Dame, 2004.
- [2] Blake W. K. "A Statistical Description of Pressure and Velocity Fields at the trailing Edge of a Flat Strut". Technical Report 4241. David W. Taylor Naval Research Center, 1975.
- [3] Quéméré P., Sagaut P. "Zonal multidomain RANS/LES simulations of turbulent flows". International Journal for Numerical Methods in Fluids, Vol. 40, pp. 903-925, 2002.
- [4] Schlüter J.U., Pitsh H., Moin P. "LES inflow conditions for coupling with Reynolds-averaged flow solvers", AIAA Journal, Vol. 42:3, pp. 478-484, 2003.
- [5] Sergent E. (2004). PhD Thesis, L'Ecole Centrale de Lyon, 2002.
- [6] Mathey F., Cokljat D., Bertoglio J.P. and Sergent E., (2003). "Specification of Inlet Boundary Condition Using Vortex Method", in Turbulence, Heat and Mass Transfer 4, Eds: K. Hanjalic, Y. Nagano and M. Tummers, Begell House Inc.
- [7] Menter. F. R. (1994). *Two-Equation Eddy-Viscosity Turbulence Models for Engineering Applications*. AIAA Journal, 32(8):1598-1605.
- [8] Fluent 6 User's Guide, Fluent Inc., Lebanon NH03766, USA, 2000.
- [9] Kim S. E., Mathur S. R., Murthy J. Y., Choudhury D. (1998). *A Reynolds Averaged Navier-Stokes Solver Using Unstructured Mesh-Based Finite-Volume Scheme*. AIAA-Paper 98-0231.
- [10] Kim S. (2004). *Large Eddy Simulation Using an Unstructured Mesh Based Finite-Volume Solver*, AIAA-Paper-2004-2548.
- [11] Smagorinsky. *General Circulation Experiments with the Primitive Equations. I: The Basic Experiment*. Monthly Weather Review, Vol. 91, pp. 99-162, 1963.
- [12] Ffowcs Williams J., Hawkins D., "Sound Generated by Turbulence and Surfaces in Arbitrary Motion", Philosophical Transactions of The Royal Society, Vol. A264, pp. 321-342, 1969.
- [13] Kato C., Lida A., Fujita H., Ikegawa M. "Numerical prediction of aerodynamic noise from low Mach number turbulent wake", AIAA Paper 1993-0145, 1993.
- [14] Shannon D. W., Morris C. S. "Visualization of blunt trailing edge turbulence", 11th International Symposium on Flow Visualization, University of Notre Dame, August 9-12, 2004.